Mon. Not. R. Astron. Soc. **312**, 853–858 (2000)

The very flat radio–millimetre spectrum of Cygnus X-1

R. P. Fender,[1★] G. G. Pooley,[2] P. Durouchoux,[3] R. P. J. Tilanus[4,5] and C. Brocksopp[6]

[1]*Astronomical Institute 'Anton Pannekoek' and Center for High Energy Astrophysics, University of Amsterdam, Kruislaan 403, 1098 SJ Amsterdam, the Netherlands*
[2]*Mullard Radio Astronomy Observatory, Cavendish Laboratory, Madingley Road, Cambridge CB3 0HE*
[3]*C.E. Saclay, DSM, DAPNIA, Service d'Astrophysique, 91191 Gif-sur-Yvette Cedex, France*
[4]*Joint Astronomy Centre, 660 N. A'ohōkū Pl., Hawaii 96720, USA*
[5]*Netherlands Foundation for Research in Astronomy, P.O. Box 2, 7990 AA Dwingeloo, the Netherlands*
[6]*Astronomy Centre, University of Sussex, Falmer, Brighton BN1 9QH*

Accepted 1999 October 18. Received 1999 August 24; in original form 1999 May 25

ABSTRACT

We present almost-simultaneous detections of Cygnus X-1 in the radio and mm regimes, obtained during the low/hard X-ray state. The source displays a flat spectrum between 2 and 220 GHz, with a spectral index $|\alpha| \leqslant 0.15$ (3σ). There is no evidence for either a low- or high-frequency cut-off, but in the mid-infrared ($\sim$30 μm) thermal emission from the OB-type companion star becomes dominant. The integrated luminosity of this flat-spectrum emission in quiescence is $\geqslant 2 \times 10^{31}$ erg s^{-1} (2×10^{24} W). Assuming the emission originates in a jet for which non-radiative (e.g. adiabatic expansion) losses dominate, this is a very conservative lower limit on the power required to maintain the jet. A comparison with Cyg X-3 and GRS 1915+105, the other X-ray binaries for which a flat spectrum at shorter than cm wavelengths has been observed, shows that the jet in Cyg X-1 is significantly less luminous and less variable, and is probably our best example to date of a continuous, steady, outflow from an X-ray binary. The emissive mechanism responsible for such a flat spectral component remains uncertain. Specifically, we note that the radio–mm spectra observed from these X-ray binaries are much flatter than those of the 'flat-spectrum' AGN, and that existing models of synchrotron emission from partially self-absorbed radio cores, which predict a high-frequency cut-off in the mm regime, are not directly applicable.

Key words: binaries: close – stars: individual: Cygnus X-1 – ISM: jets and outflows – radio continuum: stars.

1 INTRODUCTION

Cygnus X-1 (V1357 Cygni, HDE 226868) is one of the brightest X-ray binaries (XRBs) and is the classical black hole candidate (BHC); the inferred mass for the compact object is $\sim 7\,M_\odot$ (e.g. Gies & Bolton 1986). The radio emission in the low/hard X-ray state in the cm-wave band is persistent, and although it varies by a factor of about 5 the variations are much less spectacular than those of other well-studied XRBs such as Cygnus X-3 and GRS 1915+105. The radio flux is modulated at the 5.6-d orbital period, particularly at higher frequencies, and has a spectral index ($\alpha = \Delta \log S_\nu / \Delta \log \nu$) close to zero ($|\alpha| < 0.1$ between 2 and 15 GHz; Pooley, Fender & Brocksopp 1999). There are also variations on time-scales as short as 1 h and long-period fluctuations with an apparent 140-d period. The radio emission is also known to change at major state-changes in the X-ray emission (Hjellming, Gibson & Owen 1975), in the sense that it is reduced in the X-ray high/soft and/or 'intermediate' states. For long periods both the radio and X-ray emission are relatively stable, with the mean radio flux density at cm wavelengths in 1996–1998 being about 14 mJy (Pooley et al. 1999). A detailed comparison of short- and long-term behaviour from radio to hard X-rays is presented in Brocksopp et al. (1999). Stirling, Spencer & Garrett (1998) and de la Force et al. (in preparation) have resolved the radio emission from Cyg X-1 on milliarcsecond angular scales, supporting an origin in a spatially extended outflow or jet. A single previous detection of 10 ± 3 mJy at 250 GHz reported by Altenhoff, Thum & Wendker (1994), which was not simultaneous with radio observations, implied the presence of an approximately flat spectrum from cm through mm wavelengths.

In this paper we describe multiple detections of the source simultaneously at cm and mm wavelengths. These observations reveal a very flat spectrum extending from the radio to the mm regimes. They do not reveal any high-frequency cut-off in the spectrum and raise the inferred quiescent cm–mm luminosity by a factor of about 15.

★ E-mail: rpf@astro.uva.nl

2 OBSERVATIONS

2.1 Radio

Cygnus X-1 is monitored approximately daily by the Green Bank Interferometer (GBI) at 2.3 and 8.3 GHz and by the Ryle Telescope (RT) at 15 GHz. Details of typical GBI observations can be found in, for example, Waltman et al. (1994). The RT observations of Cyg X-1 are described in Pooley et al. (1999).

2.2 IRAM

The observations were carried out with the Institutde Radio-astronomie Millmetrique (IRAM) 30-m telescope at Pico Veleta (Spain) on 1997 August 4. We observed Cyg X-1 simultaneously in the HCN ($J = 1$–0) transition at 88 GHz, with the SIS 3-mm-1 receiver, in CN ($N = 1$–0) transition at 113 GHz, with the SIS 3-mm-2 receiver, in CN ($N = 2$–1) transition at 220 GHz using the R.230G1 (1-mm) receiver. The half-power beamwidths (HPBW) are, respectively, 27, 22 and 10.5 arcsec at 88, 113 and 226 GHz. The observations were taken using a position switching mode, with a reference position at -1 arcmin in RA compared to the source position. The mean system temperatures were 185, 403 and 514 K, and the opacities 0.1, 0.28 and 0.51, respectively, for the 3-mm-1, 3-mm-2 and 230G1 receivers. Due to the factor of 3 between the opacity at 88 and 113 GHz, we used the 3-mm-1 receiver, with a 512-MHz bandwidth, centred on the HCN ($J =$ 1–0) line to estimate the Cyg X-1 continuum emission. The calibration was taken on the source K3-50A, and we observed Cyg X-1 for a real time of 30 min, using 12 subscans of 20 s (10 s on source and 10 s off source). The continuum emission from Cyg X-1 was detected at a level of 15.9 mJy (3.2σ) assuming a 6 Jy K^{-1} ratio at 88.6 GHz.

2.3 JCMT

James Clerk Maxwell Telescope (JCMT) SCUBA (Holland et al. 1999) 1350- and 2000-μm photometry observations of Cyg X-1 were carried out in 1998 May. Rather than employing the arrays these observations used the longer-wavelength single-pixel bolometers positioned around the arrays. The data reduction was performed in the standard manner using SURF (Jenness 1998; Jenness & Lightfoot 1998). Photometric calibration was achieved by skydip analysis and photometry of Uranus and/or the secondary standard CRL2688. The emphasis of the observations was on 'detection' rather than accurate flux determinations; the 1350-μm flux densities have an accuracy of about 20 per cent, the 2000-μm flux densities of 25–30 per cent. The radio, IRAM and JCMT data are plotted in Fig. 1. Least-squares fitting of single power laws to the data from the two epochs results in spectral indices of 0.07 ± 0.04 and -0.06 ± 0.05 for 1997 August and 1998 May, respectively.

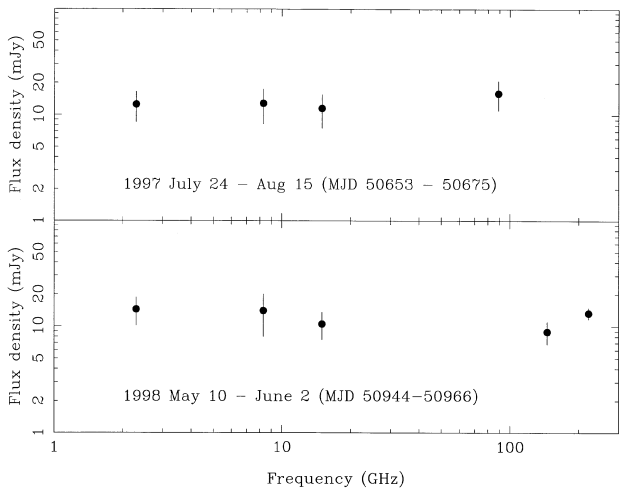

Figure 1. Mean 2–220 GHz radio/mm spectra of Cyg X-1 in 1997 August and 1998 May. The spectrum is clearly flat across two decades of frequency at both epochs (best-fitting spectral indices of 0.07 ± 0.04 and -0.06 ± 0.05 in 1997 and 1998, respectively).

2.4 *XTE*

Cyg X-1 is monitored up to several times daily in the 2–12 keV band by the *Rossi X-ray Timing Explorer* (*RXTE*) All-Sky Monitor (ASM). See, for example, Levine et al. (1996) for more details. The total flux measured by individual scans is plotted in the top panels of Fig. 2. Cyg X-1 was in the low/hard X-ray state throughout the period of these observations.

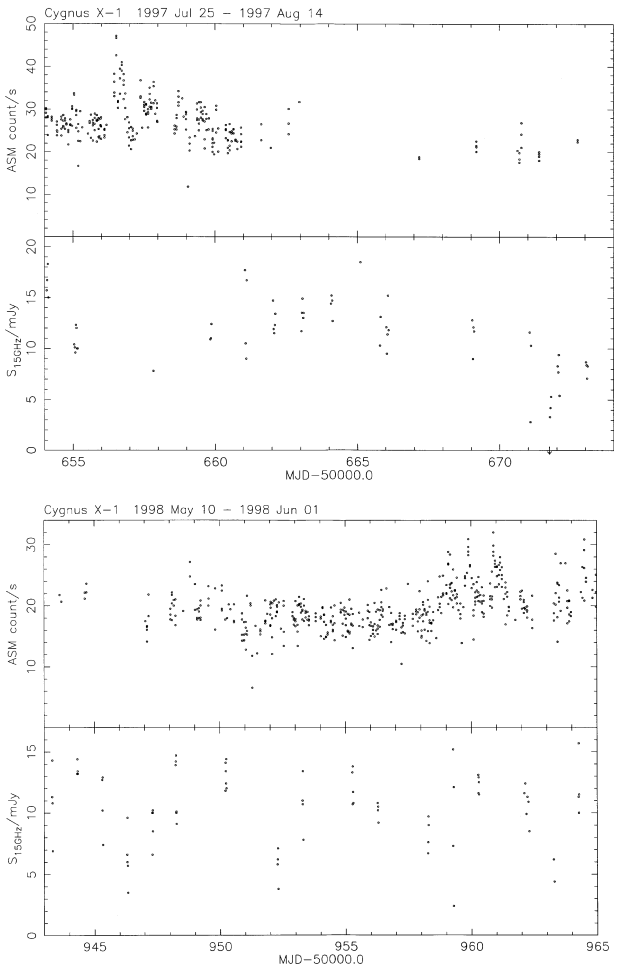

Figure 2. The variations of the 2–12 keV X-ray count rate (upper panels) and the flux density at 15 GHz (lower panels) over the two intervals during which mm-wave observation were made.

Table 1. Mean 2–220 GHz flux densities of Cyg X-1 in 1997 August and 1998 May. 'Errors' at $\nu \geqslant 89$ GHz are dominated by measurement uncertainties, whereas those at 2–15 GHz are dominated by intrinsic source variability. These data are plotted in Fig. 1.

Date (MJD)	Frequency (GHz)	Flux density (mJy)
50 664–	089	15.9 ± 4.9
50 675	015	11.5 ± 4.0
(1997 July–	8.3	12.8 ± 4.6
August)	2.3	12.5 ± 4.0
50 945–	221	13.3 ± 1.6
50 964	146	08.9 ± 2.1
(1998 May–	15	10.5 ± 3.0
June)	8.3	14.0 ± 6.0
	2.3	14.4 ± 4.2

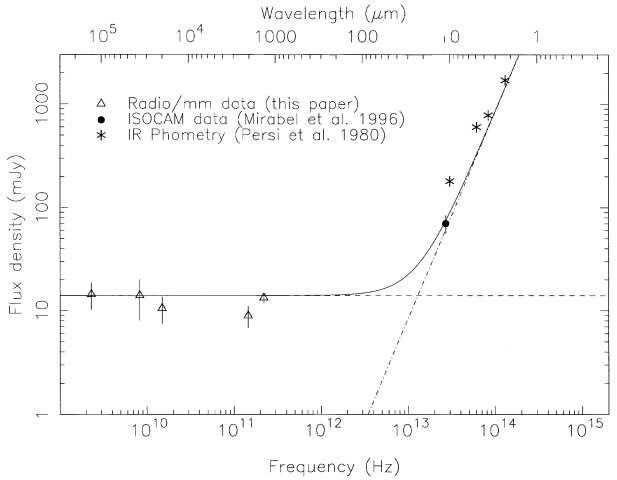

Figure 3. The broad-band spectrum of Cyg X-1 from radio to optical wavelengths, combining our radio/mm data with the ISOCAM observations of Mirabel et al. (1996) and ground-based photometry of Persi et al. (1980). It is clear that even without a high-frequency cut-off the flat spectral component will be dominated by the thermal emission from the OB supergiant at wavelengths of 30 μm or shorter.

3 DISCUSSION

3.1 Flux densities at the two epochs

Table 1 summarizes the mean flux densities observed during these two epochs. At mm wavelengths (frequencies $\geqslant$89 GHz) errors reflect measurement uncertainties; at cm wavelengths 'errors' reflect the intrinsic source variability, about which little is known at mm wavelengths.

3.2 Variability at cm and X-ray wavelengths

The variations of 15-GHz flux density and X-ray count rate during the two observing intervals concerned are shown in Fig. 2. Both intervals show some enhanced activity in the X-ray band; see the discussion in Brocksopp et al. (1999). The overall mean amplitude of the 5.6-d modulation at 15 GHz is 2.0 mJy (zero peak). Table 1 lists the rms variability at 2, 8 and 15 GHz over a period of 22 d (i.e. ~four orbital periods) centred on each of the two mm observation periods. In the light of these variations, and the absence of exactly simultaneous observations, it is possible that the spectrum in the cm–mm regime also has some short-term variations, but it is probable that the mean spectral index is close to zero up to 220 GHz.

Table 2. Comparison of cm–mm luminosities of Cyg X-1, Cyg X-3 and GRS 1915+105.

Source	S_ν (flat) (mJy)	Assumed distance (kpc)	Relative luminosity
Cyg X-1	10–15	2–3	1
Cyg X-3	50–100	7–10	20–250
GRS 1915+105	30–60	7–12	30–215

3.3 The broad-band radio–optical spectrum and a comparison with other X-ray binaries

In Fig. 3 we show an extrapolation of the flat radio–mm spectrum through the infrared spectral region, combined with published infrared flux density measurements. It is clear that at wavelengths shorter than ~30 μm, the observed emission will be dominated by the thermal component from the OB-type companion star and its wind. Clearly in Cyg X-1 even if the flat spectrum emission did extend to ~1 μm it would be extremely hard, probably impossible, to detect, being more than two orders of magnitude weaker than the thermal emission.

Only two other X-ray binaries have been detected with a flat spectrum extending from cm to shorter wavelengths. In GRS 1915+105 the flat spectrum (inferred synchrotron) oscillations are observed from 13 cm to 2 μm (e.g. Fender et al. 1997; Fender & Pooley 1998). In Cyg X-3 the flat spectrum is observed to 0.85 mm (Fender et al. 1995; Ogley et al., in preparation), and maybe also to 2 μm (Fender et al. 1996). Both of these systems are generally brighter radio sources than Cyg X-1, and yet also more distant. Table 2 compares the cm–mm luminosities of the three sources for periods when a flat spectrum is detected (i.e. Cyg X-1 in the low/hard X-ray state, GRS 1915+105 during periods of oscillations, Cyg X-3 almost all the time). It is clear that the flat-spectrum component in Cyg X-1, as well as being less variable, is also considerably less luminous than those observed from Cyg X-3 and GRS 1915+105, by at least an order of magnitude. As noted already in Fender et al. (1997) the flat-spectrum emission in Cyg X-3 and GRS 1915+105 appears to have approximately the same luminosity.

GX 339-4 is a persistent black hole candidate X-ray binary with similar radio properties to Cyg X-1 (Hannikainen et al. 1998; Fender et al. 1999 and references therein). In particular, the source displays at cm wavelengths a flat spectrum with comparable luminosity to that of Cyg X-1. We fully expect therefore that sufficiently sensitive observations should also detect a flat spectrum through the (sub)mm regime from this source. Additionally, as GX 339-4 is believed to be a low-mass X-ray binary with a less luminous companion star than in the Cyg X-1 system, we may have more chance of detecting the flat spectrum at near-infrared wavelengths.

3.4 The nature of the flat-spectrum component

Tables 1, 3 and 4 and Figs 1 and 3 summarize the observations of Cyg X-1 for 1997 August 4 and 1998 May 11–20. The source is clearly displaying a flat spectrum through the radio–mm regimes

Table 3. Log of IRAM observations of Cyg X-1 in 1997 August.

Date (MJD)	Frequency (GHz)	Flux density (mJy)
50 644	89	15.9 ± 4.9

Table 4. Log of JCMT observations of Cyg X-1 in 1998 May.

Date (MJD)	Frequency (GHz)	Flux density (mJy)
50 945.7	146	09.2 ± 3.5
50 950.8	146	05.8 ± 3.2
50 960.7	221	11.6 ± 2.1
50 964.5	146	13.2 ± 4.4
50 964.5	221	15.6 ± 2.5
All data	146	08.9 ± 2.1
–	221	13.3 ± 1.6

at both epochs. While radio emission from X-ray binaries is generally assumed to be synchrotron in origin (see e.g. Hjellming 1988; Hjellming & Han 1995), in the case of Cygnus X-1 we do not have direct observational evidence for this. Even the most rapid variability observed at 15 GHz does not require a brightness temperature in excess of 10^9 K, and there is no direct measurement of linear polarization. So, while some form of self-absorbed synchrotron emission remains a possible origin for the flat spectral component, other emissive mechanisms must also be considered.

3.4.1 Energetics

The observed luminosity of a flat-spectrum source is directly proportional to the total bandwidth. In the case of Cyg X-1, the cm–mm flat spectral component corresponds to a radiative luminosity of $\geqslant 2\times10^{31}$ erg s^{-1} (2×10^{24} W). If the emission arises in an outflow in which non-radiative (e.g. adiabatic expansion) losses dominate (which seems likely to be the case for relativistic jets from X-ray transients, see e.g. Hjellming & Han 1995) then even the integrated radiative luminosity is only a lower limit on the total power (i.e. it neglects, for example, electron acceleration and bulk kinetic energy) required to maintain the jet. Beyond the mm regime, in the infrared, thermal emission from the companion, stellar wind and accretion disc begin to dominate the spectrum of the system (Fig. 3) and it may be very difficult to ever measure any high-frequency limit to the flat spectral component emission. Note that there is strong observational evidence that the flat-spectrum oscillations observed from GRS 1915+105 are dominated by adiabatic expansion losses, based upon the similarity of the oscillation decay rates at cm and infrared wavelengths (Fender et al. 1997; Fender & Pooley 1998).

3.4.2 Partially self-absorbed synchrotron models developed for 'flat-spectrum' AGN

It is easy to draw parallels between the flat-spectrum radio–mm emission from Cyg X-1 (and also Cyg X-3 and GRS 1915+105; see above) and the 'flat-spectrum' extragalactic radio sources. These systems are generally radio-loud active galactic nuclei (AGN) in which the flat-spectrum component corresponds to the 'core' or base of the jet. As pointed out by Cotton et al. (1980) it would appear to require a 'cosmic conspiracy' of superposition of individual self-absorbed synchrotron components in order to produce a composite flat spectrum. Marscher & Gear (1985) and O'Dell et al. (1988) showed that you can more comfortably reproduce 'flat-spectrum' variability via shocks in conical jets. A conical jet model for radio emission from X-ray binaries was presented by Hjellming & Johnston (1988). Giovanoni & Kazanas (1990) suggested that energy transport by relativistic neutrons naturally explained the combination of electron spectrum, density and magnetic field profiles required to produce an observed flat synchrotron spectrum. Alternatively, Wang et al. (1997) have suggested that the flat-spectrum emission is optically thin from a flattened electron energy distribution. However, there are problems with the application of most, possibly all, of these models to the flat radio–mm(–infrared) spectra observed from Cyg X-1, Cyg X-3 and GRS 1915+105. The simultaneous radio–infrared oscillations observed in GRS 1915+105 constitute evidence against both shocks which cool via radiative losses (as the decay rate is the same at 2 cm and 2 μm) and an optically thin solution (as the infrared–radio delay, as well as delays within the radio band, suggest significant optical depth effects). Furthermore, all the conical jet and related models only predict a flat spectrum over at most three decades in frequency; the problem in all cases is the prediction of a high-frequency cut-off somewhere in the mm band. This is observed in nearly all cases for 'flat-spectrum' AGN, where the mean spectral index in the mm band is in fact $\langle\alpha_{\rm mm}\rangle = -0.75 \pm 0.05$ (Bloom et al. 1994). It is therefore clear that the three X-ray binaries in question have much flatter (consistent with completely flat) radio–mm(–infrared) spectra than the 'flat-spectrum' AGN, and the applicability of the self-absorbed synchrotron models to these X-ray binary spectra remains to be established.

If the emissive mechanism *is* synchrotron, then assuming that the mm emission is not significantly Doppler boosted, we can estimate a minimum size for the emitting region from the inverse Compton brightness temperature limit of 10^{12} K. At 220 GHz, this is only 10^{10} cm, which is relatively close to the compact object and well within the binary separation ($\sim10^{12}$ cm) of the system.

3.4.3 Alternatives to synchrotron emission?

An obvious candidate for the emissive mechanism of a flat spectral component is optically thin free–free emission. For optically thin free–free emission from a thermal plasma, we need to have a sufficiently large emission measure, whilst keeping the spectrum optically thin to $\nu \leqslant 2$ GHz. Assuming a fully ionized pure hydrogen plasma and a Gaunt factor of unity (neither of which assumptions will affect an order-of-magnitude estimate), and a distance to the system of 2.5 kpc, we find that we need to satisfy the following criteria:

$$r^3 N_{\rm e}^2 T_{\rm e}^{-1/2} \geqslant 4\times10^{56}$$

and

$$r N_{\rm e}^2 T_{\rm e}^{-3/2} \leqslant 2\times10^{20}$$

where r is the dimension of the cloud (cm) along the line of sight, $N_{\rm e}$ is the electron number density (cm^{-3}) and $T_{\rm e}$ is the electron temperature (T). The first criterion is necessary to produce the observed level of emission, the second to prevent the cloud becoming optically thick to free–free self-absorption. As a result we can determine a minimum size of a (spherical) cloud (and

corresponding N_e) for different temperatures. For a cloud of $T = 10^4$ K, i.e. in approximate thermal equilibrium with the OB star wind, $r \geqslant 10^{16}$ cm ($N_e \sim 10^6$ cm^{-3}). For a much hotter cloud of temperature 10^9 K a dimension of $r \geqslant 10^{14}$ cm ($N_e \sim 10^9$ cm^{-3}) is still required. This is very large indeed compared to the dimensions of the binary orbit, and a significantly larger emission measure than would be expected for the OB star alone. In this case the 50 per cent variability time-scale, would be $\geqslant$1 h for a 10^9 K cloud, and $\geqslant$ days for $T = 10^4$ K. The small ($1 + 4.4 \times 10^{-10} T$) correction for relativistic free–free emission is insufficient to significantly alter the result. Non-thermal optically thin free–free emission should also produce a flat spectral component, with (potentially) a greater emissivity than thermal free–free emission, but precise determination of this (including calculation of the relevant non-thermal Gaunt factors) is beyond the scope of this paper. Regardless, as noted above it is difficult to invoke a purely optically thin solution as there is evidence for frequency-dependent delays, indicating a significant optical depth.

Wright & Barlow (1975) have calculated the spectrum and flux expected from a spherically symmetric stellar wind as a result of free–free emission. Combining optically thick and optically thin regimes they predict a radio–mm spectrum with spectral index $\sim$+0.6. The flux density expected from the stellar wind of the OB-type mass donor in Cyg X-1 (assuming $\dot{M} \sim 2.5 \times 10^{-6}$ and $v_{\rm inf} \sim 2000$ km s^{-1}) would be around 0.1 mJy at 100 GHz. Therefore we can see that neither the spectrum nor flux density are compatible with the 'standard' spherically symmetric stellar wind model.

Another possibility is that the radio–mm spectrum is a combination of some emissive mechanism at radio wavelengths, probably synchrotron, with a thermal component at (sub)mm wavelengths. In the case that this thermal emission arose in an optically thick dust cloud which peaked at a frequency of $\sim 10^{13}$ Hz (30 μm), this corresponds to a temperature of $\sim$150 K for the dust cloud. At a distance of 2.5 kpc, a spherical cloud of radius $\geqslant 3 \times 10^{13}$ cm would be required. This would easily enclose the entire binary system, and presumably significantly redden the colours of the OB companion star. In addition, such a large cloud would impose a minimum time-scale for 50 per cent variability of $\geqslant$10 min. This cloud size is not infeasible for a massive OB-type companion, although in order to be in thermal equilibrium at $\sim$150 K the dust cloud would need to be much further from the star (at 10^{13} cm from the star the equilibrium temperature is likely to still be $\geqslant$1000 K).

4 CONCLUSIONS

Cyg X-1 was previously known to have a flat radio spectrum from 2 to 15 GHz (Pooley et al. 1999) with a mean flux density of $\sim$14 mJy. This corresponds to an integrated synchrotron luminosity of 10^{30} erg s^{-1}. A single previous observation at 250 GHz had implied that this flat spectrum extended to mm wavelengths (Altenhoff et al. 1994). In multiple simultaneous radio and mm observations we have confirmed the existence of a spectral component extending from cm through mm wavelengths with a very flat spectrum and no evidence of either low- or high-frequency cut-offs. Furthermore, the likelihood that adiabatic expansion losses dominate in the emitting region shows that the generation of the outflow may be far more important to the energetics of accretion in Cyg X-1 than previously suspected. Presuming the emission to arise in a jet, and comparing luminosity and variability of this component with that from Cyg X-3 and GRS 1915+105, we infer that the outflow from Cyg X-1 is considerably steadier and has a significantly lower mass flow rate. The radio–mm spectra of these X-ray binaries are much flatter than those of the 'flat-spectrum' AGN which generally peak somewhere in the mm regime and fall off rapidly in the infrared. It is not at all clear whether models of partially self-absorbed synchrotron emission from conical jets which have been developed for these AGN can be extended to apply to the much higher-frequency flat-spectrum emission we observe from Cyg X-1, Cyg X-3 and GRS 1915+105.

Detailed spectral measurements in the mm regime, preferably combined with simultaneous X-ray and radio observations, should help us to improve the currently inadequate understanding of the emission mechanisms in this unusual object. Measurement of the shortest variability time-scale (expected to be $\leqslant$1 s for non-thermal emission with a brightness temperature of 10^{12} K, $\geqslant$10 min for an optically thick dust cloud at 150 K, or $\geqslant$1 h for optically thin free–free emission) will be important in understanding the emissive mechanism. Equally important will be measurement of, or stringent upper limits to, the level of linear polarization of the flat spectral component. Finally, we predict that a flat-spectrum (sub)mm component will also be detected from the persistent black hole candidate GX 339-4 in the low/hard state.

ACKNOWLEDGMENTS

We would like to thank the referee for useful suggestions; additionally RPF would like to thank Kinwah Wu and Robert Voors for useful conversations. PD would like to thank Bertrand Lefloch for assistance with the IRAM observations. IRAM is funded by the Centre National de la Recherche Scientifique in France, the Max-Plank-Gesellschaft in Germany and the Instituto Geographico Nacional in Spain. The James Clerk Maxwell Telescope is operated by the Joint Astronomy Centre on behalf of the Particle Physics and Astronomy Research Council of the United Kingdom, the Netherlands Organisation for Scientific Research and the National Research Council of Canada. We acknowledge with thanks the use of the quick-look X-ray data provided by the ASM/*RXTE* team, and the Green Bank Interferometer data. We thank the staff at MRAO for maintenance and operation of the Ryle Telescope, which is supported by the PPARC. RPF is supported by EC Marie Curie Fellowship ERBFMBICT 972436.

REFERENCES

Altenhoff W. J., Thum C., Wendker H. J., 1994, A&A, 281, 161
Bloom S. D., Marscher A. P., Gear W. K., Terasranta H., Valtaoja E., Aller H. D., Aller M. F., 1994, AJ, 108, 398
Brocksopp C., Fender R. P., Larionov V., Lyuty V. M., Tarasov A. E., Pooley G. G., Paciesas W. S., Roche P., 1999, MNRAS, 309, 1063
Cotton W. D. et al., 1980, ApJ, 238, L123
Fender R. P., Pooley G. G., 1998, MNRAS, 300, 573
Fender R. P., Bell Burnell S. J., Garrington S. T., Spencer R. E., Pooley G. G., 1995, MNRAS, 274, 633
Fender R. P., Bell Burnell S. J., Williams P. M., Webster A. S., 1996, MNRAS, 283, 798
Fender R. P., Pooley G. G., Brocksopp C., Newell S. J., 1997, MNRAS, 290, L65
Fender R. P., Corbel S., Tzioumis A. K., Sood R., McIntyre V., Campbell-Wilson D., Durouchoux P., Harmon B. A., 1999, ApJ, 519, L165
Giovanoni P. M., Kazanas D., 1990, Nat, 345, 319
Gies D. R., Bolton C. T., 1986, ApJ, 304, 371

Hannikainen D. C., Hunstead R. W., Campbell-Wilson D., Sood R. K., 1998, A&A, 297, 556
Hjellming R. M., 1988, in Verschur G. L., Kellerman K. I., eds, Galactic and Extragalactic Radio Astronomy, A&A Library Series. Springer-Verlag, Berlin, p. 381
Hjellming R. M., Han X. H., 1995, in Lewin W. H. G., van Paradijs J., van den Heuvel E. P. J., eds, X-ray Binaries. Cambridge Univ. Press, Cambridge, p. 308
Hjellming R. M., Johnston K. J., 1988, ApJ, 328, 600
Hjellming R. M., Gibson D. M., Owen F. N., 1975, Nat, 256, 111
Holland W. S. et al., 1999, MNRAS, 303, 659
Jenness T., 1998, SURF: Reducing SCUBA Data, Starlink Bulletin 20, April, Starlink Project, CLRC
Jenness T., Lightfoot J. F., 1998, in Albrecht R., Hook R. N., Bushouse H. A., eds, ASP Conf. Ser. Vol. 145, Astronomical Data Analysis Software and Systems VII. Astron. Soc. Pac., San Francisco, p. 216–219
Levine A. M., Bradt H., Cui W., Jernigan J. G., Morgan E. H., Remillard R. A., Shirey R., Smith D., 1996, ApJ, 469, L33
Marscher A. P., Gear W. K., 1985, ApJ, 298, 114
Mirabel I. F., Claret A., Cesarsky C. J., Boulade O., Cesarsky D. A., 1996, A&A, 315, L113
O'Dell S. L. et al., 1988, ApJ, 326, 668
Persi P., Ferrari-Tonilo M., Grasdalen G., Spada G., 1980, A&A, 92, 238
Pooley G. G., Fender R. P., Brocksopp C., 1999, MNRAS, 302, L1
Stirling A., Spencer R., Garrett M., 1998, Rev., New Astron., 42, 657
Waltman E. B., Fiedler R. L., Johnston K. J., Ghigo F. D., 1994, AJ, 108, 179
Wang J., Cen X., Xu J., Qian T., 1997, ApJ, 491, 501
Wright A. E., Barlow M. J., 1975, MNRAS, 170, 41

This paper has been typeset from a TEX/LATEX file prepared by the author.